



## PAPER

[View Article Online](#)  
[View Journal](#) | [View Issue](#)


Cite this: *Green Chem.*, 2024, **26**, 4127

# Synthesis of a fully bio-based self-catalyzed hyperbranched waterborne polyurethane as a sizing agent for enhancing the interfacial properties of CF/PA6 composites†

Shengtao Dai,<sup>a</sup> Fei Yan,<sup>b</sup> Siyu Zhang,<sup>a</sup> Jiaming Guo,<sup>a</sup> Lin Zhang,<sup>a</sup> Yu Liu,<sup>a</sup> <sup>a</sup> Liu Liu<sup>\*a,c,d</sup> and Yuhui Ao<sup>\*</sup>

The scientific community has dedicated the past decade to integrate its resources in pursuit of “sustainable development”, aiming to pave the way for a perpetually eco-friendly and sustainable future. As a part of this collective effort, traditional petroleum-based polyurethanes have been progressively substituted by environmentally friendly alternatives. In this study, a conservation-minded approach was implemented using a green solvent,  $\gamma$ -valerolactone, along with fully biogenic-derived reagents: epoxidized soybean oil, tartaric acid and L-lysine diisocyanate to develop a hyperbranched waterborne polyurethane (HWPU) sizing agent. Meanwhile, tertiary amine was integrated into the polyol structure, facilitating the self-catalytic process *en route* to polyurethane, thereby eliminating the need for highly toxic catalysts. The meticulously developed fully bio-based sizing agent notably enhanced the interfacial properties between the carbon fiber (CF) and nylon 6 resin matrix. Comprehensive mechanical property evaluations of the modified composites revealed 49.4% and 49.6% improvements in flexural strength and interlaminar shear strength, respectively, compared with pristine CF composites. Additionally, interfacial shear strength tests demonstrated a substantial increase of 66.1%. This work presents an attractive avenue for the prospective industrial production and application of a green HWPU sizing agent.

Received 6th November 2023,  
Accepted 19th February 2024

DOI: 10.1039/d3gc04294d

[rsc.li/greenchem](http://rsc.li/greenchem)

## 1. Introduction

Carbon fiber-reinforced thermoplastic polymer composites (CFRTPs) have gained wide-ranging utilization across diverse industries, including medical instrumentation, construction and shipbuilding due to their exceptional attributes, such as high thermal resistance, reusability, and superior mechanical strength.<sup>1–5</sup> In the field of composite manufacturing, thermoplastic nylon 6 (PA6) is frequently selected to complement carbon fiber (CF), primarily because of its broad processing temperature range and impressive characteristics, including corrosion resistance, high tensile strength, and ease of

workability.<sup>6–9</sup> Fundamentally, the mechanical performance of CF composites is not solely determined by the inherent characteristics of their ingredient elements but also restricted by the quality of interfacial bonding between these components. Consequently, the attainment of a superior interphase is imperative to effectively endure and equitably distribute internal stresses.<sup>10</sup> Regrettably, the inherently smooth and chemically inert surface of CF often results in suboptimal interfacial properties, significantly constraining its potential applications.<sup>11</sup> To address this challenge, a multitude of surface modification techniques for fibers have been extensively deployed. These techniques encompass a range of methodologies, such as chemical vapor deposition,<sup>12</sup> surface grafting,<sup>13</sup> and sizing.<sup>14</sup> Among these approaches, appropriate sizing has emerged as a pivotal strategy in CF composite manufacturing, distinguished by its efficiency, accessibility, and noteworthy capacity for bolstering the interfacial region.<sup>15</sup> Nevertheless, it is important to note that the currently commercial CF sizing agents predominantly consist of conventional thermosetting resins, rendering them ill-suited for integration with thermoplastic resin systems and resulting in weak interfacial interactions.<sup>16</sup> Hence, there is an urgent need to explore sizing agents compatible with PA6 resin, thus fulfilling

<sup>a</sup>Jilin Provincial Laboratory of Carbon Fiber and Composites, Jilin Province Key Laboratory of Carbon Fiber Development and Application, College of Chemistry and Life Science, Changchun University of Technology, Changchun 130012, China. E-mail: [liu.liu@zju.edu.cn](mailto:liu.liu@zju.edu.cn), [aoyuhui@ccut.edu.cn](mailto:aoyuhui@ccut.edu.cn)

<sup>b</sup>College of Chemical and Material Engineering, QuZhou University, Quzhou 324000, China

<sup>c</sup>Institute of Zhejiang University-Quzhou, Quzhou, 324000, China

<sup>d</sup>College of Chemical and Biological Engineering, Zhejiang University, Hangzhou 310027, China

† Electronic supplementary information (ESI) available. See DOI: <https://doi.org/10.1039/d3gc04294d>

the imperative for robust interfacial bonding between CF and PA6 and ultimately unlocking the full potential of CFRTP composites.

Based on the selection of raw materials and the manufacturing processes employed, polyurethanes can be categorized into two types: thermoplastic and thermosetting, which exhibit a notable chemical affinity with PA6, driven by the “like-dissolves-like” principle.<sup>17</sup> This intriguing similarity has garnered significant attention, particularly in the utilization of polyurethane sizing agents to enhance the interfacial interactions between CF and PA6.<sup>18,19</sup> Traditional waterborne polyurethanes (WPU) typically feature linear structures derived from petroleum-based organic chemicals, with the manufacture often involving the use of toxic solvents and catalysts.<sup>20,21</sup> However, mounting concerns surrounding the release of volatile organic chemicals (VOCs), coupled with anxieties about the depletion of petroleum reserves and the unpredictable fluctuations in petroleum feedstock prices, have prompted innovative exploration across diverse chemical industries.<sup>22–24</sup> In response, the use of bio-based alternative reagents and bio-based polymers to enhance the interface between CF and the resin matrix is increasingly garnering attention within the academic and research communities,<sup>25–29</sup> mainly due to their abundant availability, cost-effectiveness, and environmental sustainability.<sup>30–32</sup> Consequently, a great deal of research has been dedicated to the development of bio-based WPU synthesized using green solvents, with the aim of serving a wide spectrum of applications.<sup>33</sup> Moreover, considering the toxicity of dibutyltin dilaurate (DBTDL), a commonly used catalyst to accelerate polyurethane synthesis, and the associated challenges in separating it from reaction mixtures, researchers have shifted their focus towards alternative strategies.<sup>34,35</sup> In essence, the imperative lies in the exploration of bio-derived WPU derived from a self-catalytic process to effectively eliminate the aforementioned limitations.

In addition to the DBTDL catalyst, tertiary amines such as dimethylethanolamine, 1,4-diazabicyclo[2.2.2]octane, and dimethylcyclohexylamine can also be used as catalysts in polyurethane synthesis and can significantly expedite the production process.<sup>34</sup> Besides, both academic and industrial research have made substantial efforts to enhance the sustainability of polyurethanes through the creation of various innovative bio-based polyols.<sup>36,37</sup> Notably, polyurethanes can be easily derived from renewable sources such as plant oils where unsaturated fatty acids have proven to be efficient precursors for both polyols and isocyanate monomers.<sup>38,39</sup> However, progress in the development of bio-based isocyanate monomers has been somewhat constrained and has received much less attention to date. A primary hindrance to advancing this field is the necessity of using phosgene gas to produce isocyanate molecules.<sup>38,40–42</sup>

In this study, a catalyst-free hyperbranched waterborne polyurethane (HWPU) was synthesized by replacing the conventional catalyst with a catalytic polyol derived from the ring-opening reaction of epoxidized soybean oil (ESBO) with diethylamine. Simultaneously, we employed L-lysine diisocyanate

(LDI), a biodegradable bio-based diisocyanate, renowned for its ability to prevent the formation of toxic and carcinogenic aromatic diamine by-products. Last but not least, tartaric acid (TA), a readily available and naturally sourced precursor, which has been proven to be a successful substitute for petroleum-based reagents in the synthesis of polyurethane, was used to realize the fully bio-based entity synthesis. To ensure environmental friendliness,  $\gamma$ -valerolactone ( $\gamma$ -VL) was selected as a green solvent, thereby obviating the necessity for conventional organic solvents such as acetone and *N,N*-dimethylformamide during the synthetic process. In addition, drawing from our previous experience of preparing HWPU sizing agents, this particular entity boasts exceptional fluidity, high reactivity, and excellent water solubility, making it a crucial component for efficient sizing agents. On the other hand, the hyperbranched structure enriches the concentration of hydrophilic groups, which further enhances the hydrophilic properties and numerous hydrogen bonding sites, which improves the adhesion of the resin to CF. The chemical structure of the fully bio-based HWPU was analyzed using Fourier-transform infrared (FT-IR) spectroscopy, while dynamic light scattering (DLS) was employed to assess the dispersibility of the sizing agent. Various characterizations, including tests for the fiber wettability, interfacial properties, and fracture appearances of the composites, were conducted to scientifically explore the enhancement mechanism after treatment with the HWPU sizing agent. Briefly, the experimental validation confirmed the effectiveness of the design of the fully bio-based and catalyst-free HWPU sizing agent, showcasing its potential as a promising alternative for composite manufacturing. Moreover, what amplifies its significance was the entirely bio-based sourcing of materials, markedly elevating the product's environmental compatibility and mitigating its adverse impacts, aligning seamlessly with sustainable development principles. We anticipate that the exemplary attributes of the CF/PA6 composites, coupled with their commendable economic and environmentally friendly processes, will position them as highly coveted materials across diverse sectors such as the automotive, medical devices, and sports equipment sectors.

## 2. Experimental

### 2.1 Materials

The CF fabric used in this study was sourced from Toray Co. Ltd (T300-3K, Japan), while the PA6 sheets with a thickness of 0.3 mm were obtained from Sinopec (China). The key chemicals, including L-lysine diisocyanate (LDI), tartaric acid (TA, 98% purity,  $f = 2$ ), sodium bicarbonate ( $\text{NaHCO}_3$ ), sodium chloride (NaCl), magnesium sulfate heptahydrate ( $\text{MgSO}_4 \cdot 7\text{H}_2\text{O}$ ), zinc chloride ( $\text{ZnCl}_2$ , reagent grade,  $\geq 98\%$ ), and  $\gamma$ -valerolactone ( $\gamma$ -VL), were supplied by Shanghai Macklin Biochemical Co. Ltd (China). Ethyl acetate, diethylamine, and epoxidized soybean oil (ESBO) were purchased from Aladdin Biochemical Polytron Technologies, Inc. (China).

## 2.2 Synthesis of amine-ESBO

The amine-ESBO was prepared following a previously reported method (as illustrated in Fig. 1a).<sup>43</sup> The process began with the dissolution of 7.6 g of ESBO in 6 mL of diethylamine within a round-bottom flask. Subsequently, 1.2 g of zinc chloride was added to the mixture. The temperature was carefully maintained at a constant 80 °C using an oil bath, while the solution was vigorously stirred and heated for 4 hours. After the heating phase, the mixture was allowed to cool down to 25 °C and subsequently evaporated using a rotovapor at 60 °C. Ethyl acetate was employed to dissolve the ESBO, and the resulting solution was then carefully moved into a 250 mL separatory funnel. To remove ZnCl<sub>2</sub>, a series of three washes were performed, each utilizing 100 mL of saturated NaHCO<sub>3</sub> solution. Finally, the organic layer was washed three times, each involving 100 mL of nanopure water and a saturated NaCl solution. Subsequently, the organic layer was meticulously dried using MgSO<sub>4</sub>·7H<sub>2</sub>O, followed by filtration. The resulting effluent was subjected to a one-hour evaporation at 60 °C under vacuum conditions, effectively eliminating any residual diethylamine.

## 2.3 Preparation of the HWPU sizing agent and CF/PA6 composites

The comprehensive synthetic procedures for the HWPU and the fabrication of CF/PA6 composites are provided in the ESI.† Fig. 1b displays a schematic diagram for the synthesis of the HWPU.

## 3. Results and discussion

### 3.1 Chemical structure of amine-ESBO and HWPU

FTIR spectra of the specimen (Fig. 3) displayed representative characteristic peaks of amine-ESBO, which provided the confirmation of the ZnCl<sub>2</sub>-catalyzed reaction between diethylamine and ESBO. Notably, a reduction in the epoxy (oxirane) band (848–823 cm<sup>-1</sup>) was observed, accompanied by the appearance of a new broad band centered at 3345 cm<sup>-1</sup>, indicating the incorporation of hydroxyl groups from the catalytic opening and elimination of oxirane rings by diethylamine.<sup>43</sup> Additionally, a novel peak at 1561 cm<sup>-1</sup> appeared, suggesting the formation of carboxyl salts during the reaction. The alterations around 2727 cm<sup>-1</sup> arose from intermolecular H-bonding interactions involving –OH and –NH<sub>2</sub>. These interactions also contributed to the visual increase in viscosity of the reaction product. The results from the <sup>1</sup>H nuclear magnetic resonance (NMR) measurements, <sup>13</sup>C NMR and high-resolution mass spectra, presented in the ESI,† provided valuable insights into the chemical structure of the amine-ESBO. The obtained conclusions serve as confirmation of the successful production of amine-ESBO.

The chemical composition of HWPU was confirmed through FT-IR analysis. As depicted in Fig. 2, the amidogen moiety exhibited two distinctive peaks at 3342 cm<sup>-1</sup> and 1546 cm<sup>-1</sup>. The characteristic peak for isocyanate normally at 2250–2260 cm<sup>-1</sup> was entirely absent, indicating its complete consumption in the reaction.<sup>44,45</sup> An additional prominent peak at 1630 cm<sup>-1</sup> corresponded to the carbonyl stretching vibration of the ureido functional group, confirming the chemical transformation involving hydroxyl and isocyanate groups. Furthermore, the absorption

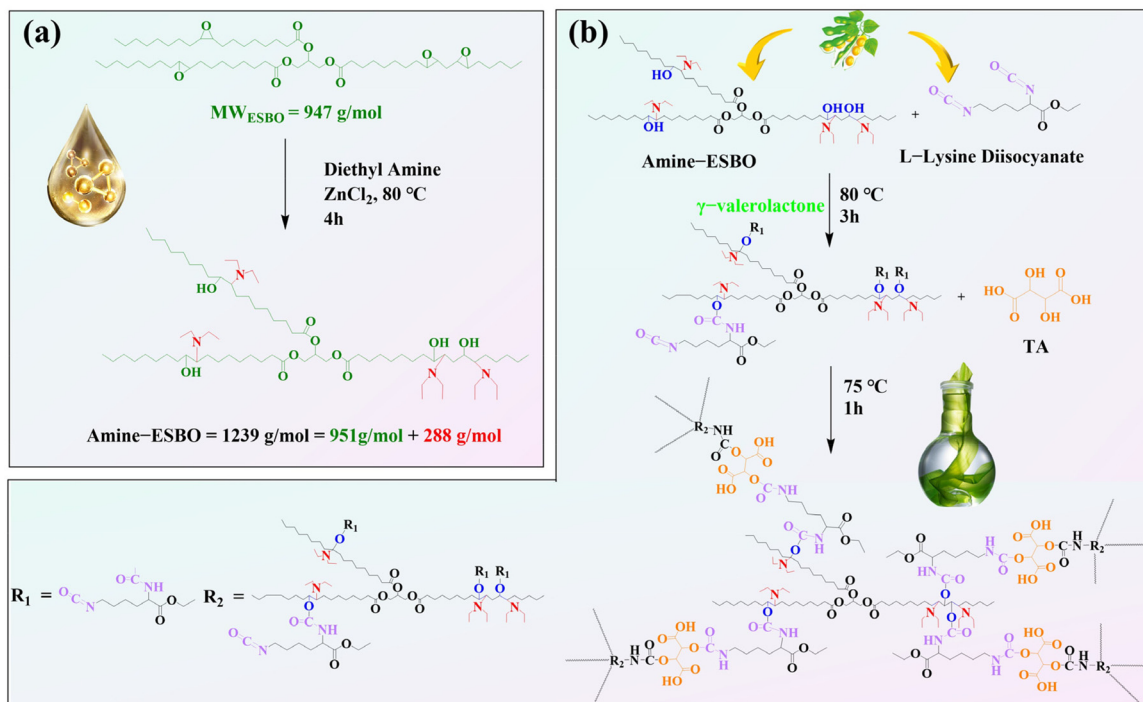


Fig. 1 Schematic diagrams showing the syntheses of (a) amine-ESBO and (b) hyperbranched polyurethane.

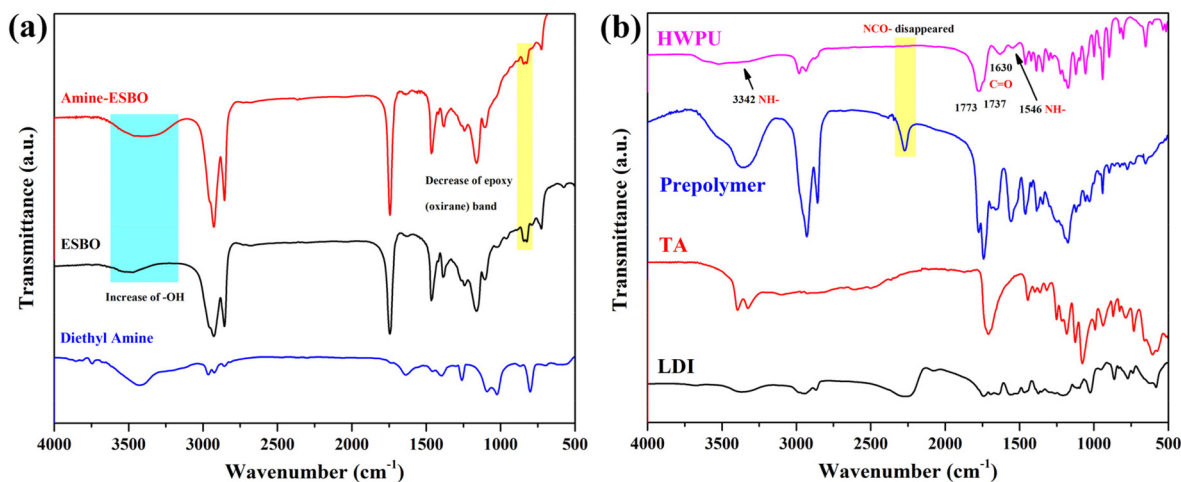


Fig. 2 FT-IR spectra of (a) ESBO, amine-ESBO, and diethyl amine and (b) HWPU, prepolymer, TA, and LDI.

bands at 1773 and 1737  $\text{cm}^{-1}$  could be attributed to the asymmetric stretching vibrations of the ester groups resulting from the neutralization of carboxylic groups by TEA during the reaction with TA.<sup>46</sup> These findings verified that the synthesized HWPU conformed to the expected structure.

### 3.2 Determination of the biomass content

To estimate the quantity of biomass integrated per gram of HWPU sizing agent manufactured using the fully bio-based raw materials detailed earlier (sourced from LDI, TA, and amine-ESBO), we first calculated the biomass content (BC, expressed as wt%) within these systems, considering LDI, TA, and ESBO as sources of renewable carbon.<sup>30</sup> Moreover, only the initial ESBO atoms that persisted in amine-ESBO were deemed biomass, as its structure underwent alteration through the inclusion of non-biomass-derived compounds (green structures in Fig. 1a denote atomic groups considered as bio-based for the calculation of the BC). The contents of LDI ( $m_{\text{LDI}}$ ), TA ( $m_{\text{TA}}$ ) and amine-ESBO ( $m_{\text{Amine-ESBO}}$ ) in HWPU were determined based on the mass ratio used for the synthesis and assuming 1 g of HWPU ( $m_{\text{HWPU}}$ ) as the basis of the calculus. Once  $m_{\text{LDI}}$ ,  $m_{\text{TA}}$ , and  $m_{\text{Amine-ESBO}}$  were known, the moles of amine-ESBO ( $\text{mol}_{\text{Amine-ESBO}}$ ) incorporated in the formulation were calculated from its molecular weight (1239  $\text{g mol}^{-1}$ ) using eqn (1). From  $\text{mol}_{\text{Amine-ESBO}}$ , the content of biomass present in amine-ESBO ( $m_{\text{Amine-ESBObio}}$ ) from the original structure of ESBO was calculated based on the remaining molecular weight of the original bonds (951  $\text{g mol}^{-1}$ ) using eqn (2). Finally, once  $m_{\text{LDI}}$ ,  $m_{\text{TA}}$ , and  $m_{\text{Amine-ESBObio}}$  were known, the BC content was calculated using eqn (3).

$$\text{mol}_{\text{Amine-ESBO}} = \frac{m_{\text{Amine-ESBO}}}{M_{\text{Amine-ESBO}}} = \frac{m_{\text{Amine-ESBO}}}{1239} \quad (1)$$

$$\begin{aligned} m_{\text{Amine-ESBObio}} &= \text{mol}_{\text{Amine-ESBO}} \cdot M_{\text{Amine-ESBObio}} \\ &= \text{mol}_{\text{Amine-ESBO}} \cdot 951 \end{aligned} \quad (2)$$

$$\text{BC}(\%) = \frac{m_{\text{LDI}} + m_{\text{TA}} + m_{\text{Amine-ESBObio}}}{m_{\text{HWPU}}} \times 100 \quad (3)$$

In accordance with this, it was determined that a remarkable 90% of the biomass weight was incorporated into the ultimate HWPU sizing agent. Compared with prior research outcomes where bio-based raw materials served as either the isocyanate precursor or bio-based polyols,<sup>47,48</sup> the notably higher biomass content observed in our system further underscores its potential as an exceptionally eco-friendly bio-based HWPU sizing agent.

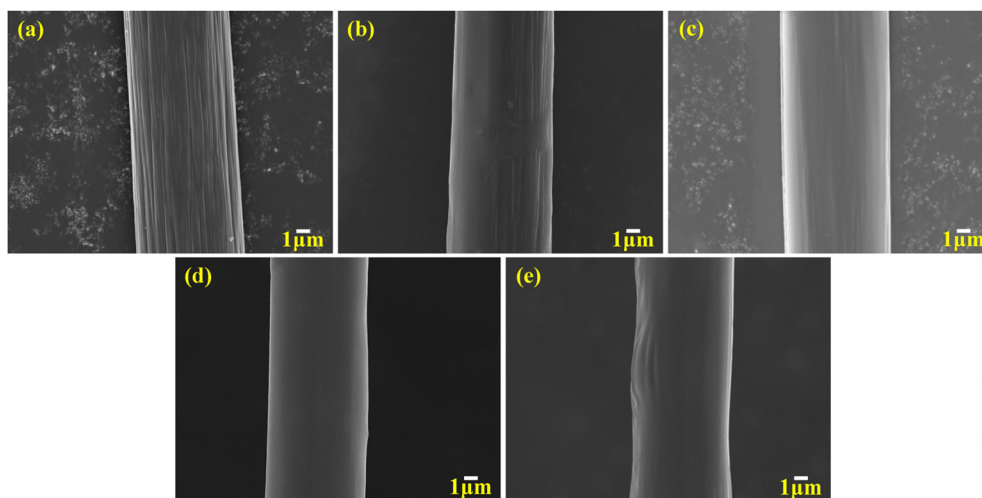
### 3.3 Surface morphology and chemical compositions of the various-sized CF

Fig. 3 illustrates the surface morphologies of the various CF samples, including untreated CF and CF sized with various concentrations of sizing agents (CF-0.5, 1.0, 1.5, and 2.0 wt%). The untreated CF sample (Fig. 3a) exhibited a rugged surface with numerous deep grooves. As the HWPU sizing agent concentration increased, the grooves on the CF were gradually enveloped by the HWPU sizing agents in CF-0.5 wt% and 1.0 wt% (Fig. 3c and d). For the CF-1.5 wt% sample (Fig. 3e), CF was uniformly coated with a consistent layer of sizing agent, leaving no exposed areas. However, noticeable excess slurry coagulation was observed on the surface of CF-2.0 wt% (Fig. 3f), which could possibly impair the adhesion performance of the composites.

### 3.4 Surface wettability of the CF

The impact of the HWPU sizing agent on the CF surface wettability was assessed through dynamic contact angle and surface energy measurements (Table 1). Following the sizing treatment, both the contact angles for deionized water and diiodomethane exhibited significant reductions, decreasing from 79.43° and 55.57° to 48.58°, and 39.88°, respectively. These decreases indicated a notable improvement in the surface wettability. The surface energies of the unsized and sized fibers increased from 36.81  $\text{mN m}^{-1}$  to 58.60  $\text{mN m}^{-1}$ ,





**Fig. 3** SEM micrographs of CF surfaces subjected to varying concentrations of HWPU sizing agent: (a) unsized, (b) 0.5 wt%, (c) 1.0 wt%, (d) 1.5 wt%, and (e) 2.0 wt%.

**Table 1** Wettability of the CF following treatment with various concentrations of HWPU sizing agent

Samples	Contact angles (°)		Surface energy (mN m <sup>-1</sup> )		
	$\theta_{\text{deionized water}}$	$\theta_{\text{diiodomethane}}$	$\gamma^{\text{d}}$	$\gamma^{\text{p}}$	$\gamma$
Unsize fibers	79.43	55.57	31.12	5.69	36.81
0.5 wt%	57.28	46.17	36.38	15.28	51.66
1.0 wt%	53.16	44.02	37.53	17.20	54.73
1.5 wt%	49.95	41.02	39.10	18.40	57.50
2.0 wt%	48.58	39.88	39.67	18.93	58.60

with the polar constituent rising from 5.69 mN m<sup>-1</sup> to 18.93 mN m<sup>-1</sup>. The application of the polyurethane introduced numerous oxygen-containing functional groups such as carboxyl and amide units to the CF surface, ultimately enhancing its surface energy and wettability, thereby fostering a robust interaction between the CF and the PA6 matrix.<sup>49,50</sup>

### 3.5 Mechanical properties of the composites

Tests of the flexural strength, interlaminar shear strength (ILSS), and interfacial shear strength (IFSS) were performed to evaluate the interfacial performance of the composites. Fig. 4 shows there was a significant enhancement in mechanical properties with increasing the concentration of HWPU sizing agent in the composites. Notably, the CF-1.5 wt% composites displayed remarkable results with a bending strength at 608.7 MPa and modulus of 37.6 GPa, representing substantial improvements of 49.4% and 36.4%, respectively, compared with the unsized CF/PA6 composites. These enhancements were attributed to the formation of a robust interface resulting from the introduction of the HWPU sizing agent, which limited matrix exfoliation. Specifically, the ILSS and IFSS values for the composites reinforced with 1.5 wt% CF showed significant increases, reaching 60.3 MPa and 68.2 MPa from

the initial values of 40.3 MPa and 41.1 MPa, respectively. These increments represented noteworthy surges of 49.6% and 66.1% compared with the unsized CF composites. However, it is important to note that excessive clustering of the sizing agent (2.0 wt%) on the CF surface adversely affected the interfacial properties and overall mechanical performance of the composites. Additionally, the assessment of the EP-sized CF composites was conducted with an aim to emphasize the significant improvements facilitated by the prepared sizing agent. Compared with both the unmodified CF/PA6 and HWPU-sized CF/PA6 composites, the compromised flexural strength and interlaminar shear strength in these composites were assigned to the suboptimal compatibility between the epoxy resin sizing agent and PA6 matrix. This incompatibility resulted in weaker interfacial adhesion and inferior mechanical performance.<sup>16</sup> In summary, these results underscore the substantial and positive impact of the HWPU sizing agent on the interfacial properties of the composites. Next, radar charts were constructed to compare the comprehensive mechanical properties of our samples against those of analogous studies (Fig. 5, based on the percentage enhancement in performance relative to the original composite materials). The thermal stability data for the sizing agents presented in this study are included in the ESI.† The bio-content of the sizing agent was quantified by evaluating the compositions of the selected raw materials used in the synthesis of the sizing agent in each work. Significantly, excluding thermal stability, the findings from this study consistently demonstrated superior values across all parameters relative to the comparative samples, as corroborated by the presented data.<sup>8,51–53</sup>

### 3.6 Fractured surface morphology of the composites

To study the reinforcing effect of the sizing agent, ILSS and IFSS tests were carried out and the fracture morphology was examined. In Fig. 6a, it can be seen that the unsized CF com-

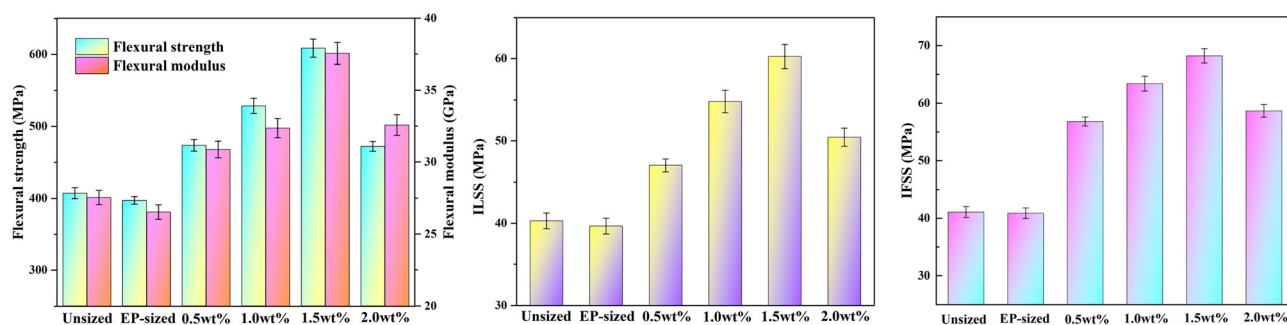


Fig. 4 Flexural strength, ILSS and IFSS values of different CF/PA6 composites.

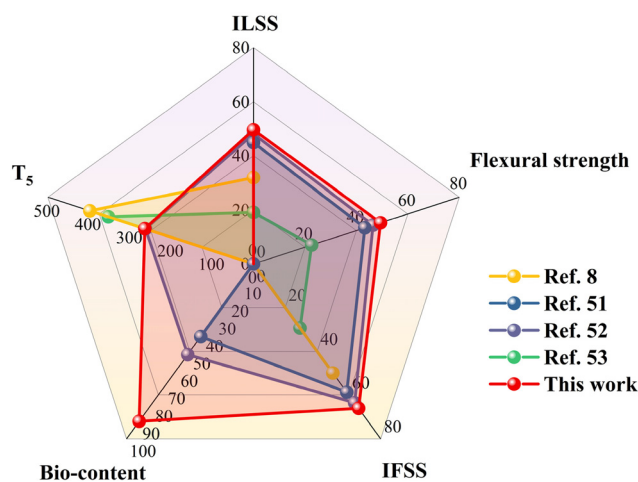


Fig. 5 Radar plot for qualitatively comparing five key aspects: ILSS, flexural strength, and IFSS for the composites, the thermal decomposition temperatures at 5% weight loss ( $T_5$ ), and bio-contents for the prepared sizing agents.

posites displayed uprooted fibers and a surface that was remarkably smooth and clean. Concurrently, as depicted in Fig. 6f, the fibers were entirely detached, leaving no discernible traces of resin. In contrast, the CF composites treated with incremental concentrations of sizing agent exhibited a pro-

nounced improvement in their interfacial performance. This enhancement could be primarily attributed to the introduction of abundant oxygen-functionalized groups such as carbamate, which significantly augmented the surface energy of the CFs compared with that of the unsize fibers. When the concentration of the HWPU sizing agent was gradually increased, the resin tightly adhered to the CF, as evidenced by the composites sized with 0.5 wt% and 1.0 wt% concentrations of HWPU (Fig. 6b and c). Furthermore, the debonded areas on the CF surface following the IFSS tests were also found to be encased in residual resin fragments (Fig. 5g and h). However, the presence of cracks and holes upon fracturing and extracting the CF from the PA6 matrix underscored instances of interface failure, representing a vulnerability in the composites (Fig. 6b and c). Remarkably, Fig. 6d shows there was a significant improvement in the CF modified with 1.5 wt% concentration of HWPU. The CF was ideally encased by the resin, resulting in reduced debonding. The fractured CF displayed a uniformly distributed cross-section intertwined with the resin, and a large amount of residual resin enveloped the debonded area, signifying superior interaction between the CF and PA6 resin (Fig. 6i). These results originated from the enhanced wettability and surface energy, along with favorable van der Waals forces and mechanical interactions between the carbon fiber and PA6 facilitated by uniform resin infiltration. Furthermore, the introduction of carbamate molecular groups through the

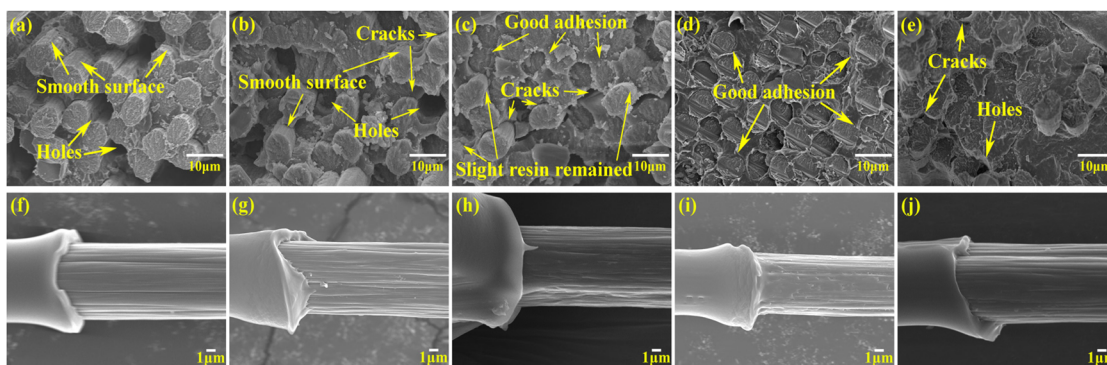


Fig. 6 SEM micrographs of the fracture morphologies of the composites after ILSS examination (a–e) and IFSS tests (f–j). CF-0 wt% (a and f), CF-0.5 wt% (b and g), CF-1.0 wt% (c and h), CF-1.5 wt% (d and i), and CF-2.0% (e and j).

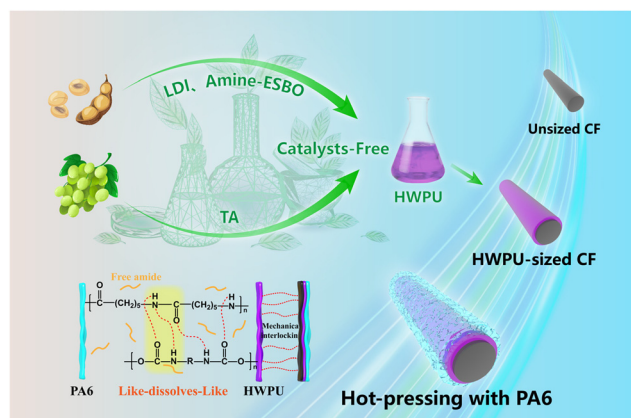


Fig. 7 Schematic representation of the sizing reinforcement mechanism in the CF/PA6 composites.

HWPU coating exhibited a striking similarity to the amide group in PA6, creating a harmonious interface between the treated CF and PA6 resin based on the “like-dissolves-like” principle. Moreover, the interfacial interaction was further enhanced by the formation of hydrogen bonds between the carbamate and amide groups in polyurethane and PA6.<sup>51</sup> However, the use of an extortionate concentration of HWPU sizing agent (2.0 wt%) (Fig. 6e and j) adversely damaged the uniformity of the coating, impeding the infiltration of the resin matrix into the CF. Consequently, the interface adhesion between the CF and PA6 was weakened, resulting in suboptimal physical properties. This study elucidated the positive impact of the HWPU sizing agent on the adhesion performance of CF with PA6 resin. The reinforcement mechanism governing the interfacial properties is depicted in Fig. 7.

## 4. Conclusions

In summary, a fully bio-based and catalyst-free HWPU sizing agent was successfully developed to enhance the interfacial properties of CF/PA6 composites. In this study, all the solvents and raw materials used for the polyurethane synthesis were of bio-origin, significantly reducing the production costs and potential health impacts on researchers. Leveraging the natural high crosslinking density of bio-based polyol-ESBO and TA, the thermal stability and functional group contents of the synthesized polyurethane resins were significantly enhanced, which not only meets the processing temperature requirements but also introduces more oxygen-containing functional groups to the CF surface during sizing, improving the bonds between the fiber and the resin matrix. The selected green solvent,  $\gamma$ -VL, exhibited excellent water solubility and non-toxicity, eliminating VOC emissions during the polyurethane preparation process. Of noteworthy significance was the consequential 49.4% and 49.6% augmentation in the maximum flexural strength and ILSS, respectively, along with a commendable 66.1% increase in IFSS for the CF-1.5 wt%/PA6

composites compared to their unsized CF/PA6 composite counterparts. Furthermore, the utilization of  $\gamma$ -VL as a green solvent further bolsters the environmental sustainability of the synthetic process. This straightforward and highly effective method holds significant promise for the industrial manufacture of CF/PA6 composites. More importantly, it offers invaluable insights into the advancement of bio-based polyurethane sizing agents, contributing significantly to a more eco-conscious and sustainable future.

## Author contributions

Shengtao Dai: Formal analysis, conceptualization, writing – original draft. Fei Yan: Formal analysis. Siyu Zhang: Formal analysis. Jiaming Guo: Investigation. Lin Zhang: Data curation, resources. Yu Liu: Investigation. Liu Liu: Conceptualization, data curation, methodology, resources, supervision, writing – original draft, writing – review & editing. Yuhui Ao: Supervision.

## Conflicts of interest

The authors declare that they have no conflicts of interest in this work. We declare that we do not have any commercial or associative interest that represents a conflict of interest in connection with the work submitted.

## Acknowledgements

This work was supported by the National Key R&D Program of China (Grant No. 2020YFB1505700), Department of Science and Technology Development Program of People's Government of Jilin Province (Grant No. 20200201189JC).

## References

- 1 J. Chen, K. Wang and Y. Zhao, *Compos. Sci. Technol.*, 2018, **154**, 175–186.
- 2 B.-G. Cho, J.-E. Lee, S.-H. Hwang, J. H. Han, H. G. Chae and Y.-B. Park, *Composites, Part A*, 2020, **135**, 105938.
- 3 X. Gao, Z. Huang, H. Zhou, D. Li, Y. Li and Y. Wang, *Polym. Compos.*, 2019, **40**, 3749–3757.
- 4 N. Li, L. Zong, Z. Wu, C. Liu, X. Wang, F. Bao, J. Wang and X. Jian, *Composites, Part A*, 2017, **101**, 490–499.
- 5 X. Ma, J. Guo, S. Wen, Y. Liu, J. Wang, L. Zhao, Y. Ao, L. Liu and F. Yan, *Adv. Mater. Interfaces*, 2022, **9**, 2201220.
- 6 N. Karakaya, M. Papila and G. Özkoç, *Composites, Part A*, 2020, **139**, 106106.
- 7 S. Kobayashi, T. Tsukada and T. Morimoto, *Composites, Part A*, 2017, **101**, 283–289.
- 8 N. Sun, B. Zhu, X. Cai, L. Yu, X. Yuan and Y. Zhang, *Appl. Surf. Sci.*, 2022, **599**, 153889.

- 9 D. Zhao, H. Hamada and Y. Yang, *Composites, Part B*, 2019, **160**, 535–545.
- 10 L. Shi, G. Song, P. Li, X. Li, D. Pan, Y. Huang, L. Ma and Z. Guo, *Compos. Sci. Technol.*, 2021, **201**, 108522.
- 11 L. Liu, F. Yan, M. Li, M. Zhang, L. Xiao, L. Shang and Y. Ao, *Composites, Part A*, 2018, **114**, 418–428.
- 12 D. Wu, Z. Yao, X. Sun, X. Liu, L. Liu, R. Zhang and C. Wang, *Chem. Eng. J.*, 2022, **429**, 132449.
- 13 L. Liu, F. Yan, M. Li, M. Zhang, L. Xiao, L. Shang and Y. Ao, *Composites, Part A*, 2018, **107**, 616–625.
- 14 S. Dai, P. Li, X. Li, C. Ning, L. Kong, L. Fang, Y. Liu, L. Liu and Y. Ao, *Compos. Commun.*, 2021, **27**, 100849.
- 15 Y. Dong, Y. Zhu, Y. Zhao, F. Liu, E. Wang and Y. Fu, *Composites, Part A*, 2017, **102**, 357–367.
- 16 H. Yuan, S. Zhang and C. Lu, *Appl. Surf. Sci.*, 2014, **317**, 737–744.
- 17 C. Liu, B. Xiang, Y. Liu, Q. Huang, Y. Yang, S. Chen, G. Bai, Q. An, J. Cao, S. Zheng and C. Wang, *Prog. Org. Coat.*, 2016, **90**, 1–9.
- 18 Y. Yang, Z. Zhang, Y. Ma, M. Ueda, T. Yokozeki, T. Sugahara and H. Hamada, *J. Thermoplast. Compos. Mater.*, 2017, **31**, 408–425.
- 19 T. Zhang, Y. Zhao, H. Li and B. Zhang, *J. Appl. Polym. Sci.*, 2017, **10**, 46111.
- 20 Y. Han, J. Hu and Z. Xin, *Prog. Org. Coat.*, 2019, **130**, 8–16.
- 21 L. Ma, L. Song, H. Wang, L. Fan and B. Liu, *Prog. Org. Coat.*, 2018, **122**, 38–44.
- 22 N. G. R. Ivan Hevus, S. Tymoshenko, S. N. Raja and D. C. Webster, *ACS Sustainable Chem. Eng.*, 2020, **8**, 5750–5762.
- 23 P. M. Paraskar, M. S. Prabhudesai, V. M. Hatkar and R. D. Kulkarni, *Prog. Org. Coat.*, 2021, **156**, 106267.
- 24 C. Zhang, S. A. Madbouly and M. R. Kessler, *ACS Appl. Mater. Interfaces*, 2015, **7**, 1226–1233.
- 25 L. Chen, Y. Du, Y. Huang, F. Wu, H. M. Cheng, B. Fei and J. H. Xin, *Composites, Part A*, 2016, **88**, 123–130.
- 26 L. Fang, T. Qiu, Q. Yang, L. Kong, F. Yan, M. Zhang, Y. Liu, L. Liu and Y. Ao, *Compos. Commun.*, 2021, **23**, 100591.
- 27 W. Liu, Y. Wang, P. Wang, Y. Li, Q. Jiang, X. Hu, Y. Wei, Y. Qiu, S. I. S. Shahabadi and X. Lu, *Composites, Part B*, 2017, **113**, 197–205.
- 28 B. Qiu, M. Li, X. Zhang, Y. Chen, S. Zhou, M. Liang and H. Zou, *Mater. Chem. Phys.*, 2021, **258**, 123677.
- 29 M. Zhang, L. Jin, Y. Zhai, C. Cheng, F. Yan, Y. Liu, L. Liu and Y. Ao, *Compos. Commun.*, 2021, **26**, 100790.
- 30 C. A. Juan Carlos de Haro, A. T. Smit, S. Turri, P. D'Arrigo and G. Griffini, *ACS Sustainable Chem. Eng.*, 2019, **7**, 11700–11711.
- 31 L. Sougrati, S. Wendels, S. Dinescu, L.-R. Balahura, L. Sleiman and L. Avérous, *Sustainable Mater. Technol.*, 2023, **37**, e00656.
- 32 X. Zhao, T. Shou, R. Liang, S. Hu, P. Yu and L. Zhang, *Ind. Crops Prod.*, 2020, **154**, 112619.
- 33 L. Germán-Ayuso, J. M. Cuevas, R. Cobos, A. Marcos-Fernández and J. L. Vilas-Vilela, *Prog. Org. Coat.*, 2022, **173**, 107218.
- 34 A. Rahimi, A. Farhadian, L. Guo, E. Akbarinezhad, R. Sharifi, D. Irvani, A. Asghar Javidparvar, M. A. Deyab and M. A. Varfolomeev, *J. Ind. Eng. Chem.*, 2023, **123**, 170–186.
- 35 Z. Liu, B. Wu, Y. Jiang, J. Lei, C. Zhou, J. Zhang and J. Wang, *Polymer*, 2018, **143**, 129–136.
- 36 H. Luo, Y. Liu, B. Ruj, L. Sun, J. Wang and Y. He, *Int. J. Polym. Anal. Charact.*, 2021, **27**, 52–70.
- 37 H. Li, N. Mahmood, Z. Ma, M. Zhu, J. Wang, J. Zheng, Z. Yuan, Q. Wei and C. Xu, *Ind. Crops Prod.*, 2017, **103**, 64–72.
- 38 S. Lemouzy, A. Delavarde, F. Lamaty, X. Bantreil, J. Pinaud and S. Caillol, *Green Chem.*, 2023, **25**, 4833–4839.
- 39 I. Omrani, A. Farhadian, N. Babanejad, H. K. Shendi, A. Ahmadi and M. R. Nabid, *Eur. Polym. J.*, 2016, **82**, 220–231.
- 40 O. Akay, C. Altinkok, G. Acik, H. Yuce and G. K. Ege, *Eur. Polym. J.*, 2021, **161**, 110856.
- 41 J. Han, R. W. Cao, B. Chen, L. Ye, A. Y. Zhang, J. Zhang and Z. G. Feng, *J. Biomed. Mater. Res., Part A*, 2011, **96**, 705–714.
- 42 Y. Zhang, J. Liao, X. Fang, F. Bai, K. Qiao and L. Wang, *ACS Sustainable Chem. Eng.*, 2017, **5**, 4276–4284.
- 43 A. A. Atanu Biswas, S. H. Gordon, S. Z. Erhan and J. L. Willett, *J. Agric. Food Chem.*, 2005, **53**, 9485–9490.
- 44 G. Cui, W. Xia, G. Chen, M. Wei and J. Huang, *J. Appl. Polym. Sci.*, 2007, **106**, 4257–4263.
- 45 A. K. Mishra, D. K. Chattopadhyay, B. Sreedhar and K. V. S. N. Raju, *Prog. Org. Coat.*, 2006, **55**, 231–243.
- 46 B. Fernández-d'Arlas, J. A. Ramos, A. Saralegi, M. Corcuera, I. Mondragon and A. Eceiza, *Macromolecules*, 2012, **45**, 3436–3443.
- 47 F. Avelino, I. P. Miranda, T. D. Moreira, H. Becker, F. B. Romero, C. A. K. Taniguchi, S. E. Mazzetto and M. de Sá Moreira de Souza Filho, *J. Coat. Technol. Res.*, 2018, **16**, 449–463.
- 48 S. E. Klein, J. Rumpf, P. Kusch, R. Albach, M. Rehahn, S. Witzleben and M. Schulze, *RSC Adv.*, 2018, **8**, 40765–40777.
- 49 D. Jiang, L. Xing, L. Liu, X. Yan, J. Guo, X. Zhang, Q. Zhang, Z. Wu, F. Zhao, Y. Huang, S. Wei and Z. Guo, *J. Mater. Chem. A*, 2014, **2**, 18293–18303.
- 50 F. Liu, Z. Shi and Y. Dong, *Composites, Part A*, 2018, **112**, 337–345.
- 51 S. Dai, F. Yan, J. Guo, M. Li, Y. Zhao, Y. Liu, L. Liu and Y. Ao, *Compos. Sci. Technol.*, 2023, **242**, 110214.
- 52 S. Dai, F. Yan, J. Ma, J. Guo, H. Hu, Y. Liu, L. Liu and Y. Ao, *Compos. Sci. Technol.*, 2024, **245**, 110328.
- 53 C. Yan, Y. Zhu, D. Liu, H. Xu, G. Chen, M. Chen and G. Cai, *Composites, Part B*, 2023, **258**, 110675.